Full Paper

Israel Journal of Chemistry

DOI: 10.1002/ijch.201400212

Enhanced Thermal Stability of Inverted Polymer Solar Cells with Pentacene

Feng Yang,[a] Jae-Hyoung Kim,[a] Ziyi Ge,[b] and Yong-Sang Kim*[a]

Abstract: In this study, we focused on the thermal stability of organic solar cells based on poly(3-hexylthiophene) (P3HT) and (6,6)-phenyl C_{61}-butyric acid methyl ester (PCBM), fabricated by blends of P3HT:PCBM:pentacene. Enhanced thermal stability of organic solar cells was achieved by introducing pentacene (Pc) into blends of P3HT:PCBM in organic solar cells with the structure indium tin oxide/ZnO/P3HT:PCBM:Pc/poly(3,4-ethylenedioxythiophene):polystyrene sulfonate/Ag (ITO/ZnO/P3HT:PCBM:Pc/PEDOT:PSS/Ag). The donor-acceptor interfaces of devices with Pc were more stable than those without Pc in the active layer. During the thermal annealing process, the Pc in the P3HT:PCBM blends suppressed the crystallization of P3HT and PCBM, which was confirmed by optical microscopic images and UV-visible absorption spectra. The power conversion efficiency (PCE) of the device with Pc was reduced to no less than 70% of its original efficiency after keeping it at 120 °C for 24 hours, while that of the non-Pc device was reduced to 13% of its original efficiency after 24 hours at the same temperature. Based on these results, we propose a new Pc-blended organic solar cell that has advantages in the thermal annealing process.

Keywords: pentacene · photoconduction · polymers · solar cells · thermal stability

1 Introduction

Fabricated by cost-effective solution processing, polymer solar cells have attracted considerable attention in the last decade.[1] The performance of polymer solar cells has been improved by new organic materials, device engineering, and manufacturing processes. The PCE of organic solar cells is 8–11% with new materials and novel device structure.[2,3] There are two important factors for organic solar cells – efficiency and stability. The inverted structure of polymer solar cells has caught wide attention because of its good performance in efficiency and stability.

Thermal stability is one of the important aspects of inverted polymer solar cells, and the active layer is a key contributor to this stability. The active layer of polymer solar cells is composed of a polymer donor and a fullerene-derived acceptor. The layer has the tendency to rapidly coarsen when annealed above its glass transition temperature.[4] The distribution of donor and acceptor molecules is crucial for maximizing the photovoltaic performance. The phase separation of donor and acceptor domains improves charge transport to the electrodes. A large contact area between donor and acceptor aids hole-electron pair generation, and thus, a finely interpenetrating donor-acceptor network is favored in the active layer. The interpenetrating donor-acceptor networks and the phase separation are very sensitive to thermal treatments. Elevated processing and operating temperatures are real challenges to the thermal stability of inverted polymer solar cells, which must be solved prior to practical applications. Typically during the thermal treatment process, the distribution of the fullerene material in the blend is very difficult to control.

The fullerene derivative PCBM has a glass transition temperature of about 110–140 °C.[5,6] It is very important to fix the phase separation between PCBM and the polymer after evaporation of the processing solvent. However, above glass transition temperature, fullerene molecules start to slowly aggregate and form micrometer-sized crystals.[4,7,8] Overgrown crystals of PCBM cause a dramatic decrease in PCE.[9,10] Many research groups have explored strategies to control the donor-acceptor interfaces in the active layer. The first approach involves cross-linking reactions of the polymer[11,12] or fullerene[13,14] in the active layer. The cross-linked molecules prevent further coarsening of the polymer and fullerene phases and improve thermal stability. However, cross-linking reactions

[a] F. Yang, J.-H. Kim, Y.-S. Kim
School of Electronic and Electrical Engineering
Sungkyunkwan University
Suwon, Gyeonggi 440-746 (Republic of Korea)
Tel.: (+82) 31-299-4323
Fax: (+82) 31-290-7179
e-mail: yongsang@skku.edu

[b] Z. Ge
Ningbo Institute of Materials Technology & Engineering
Chinese Academy of Sciences
Ningbo 315201 (The People's Republic of China)

require chemical modifications that increase the structural complexity of the employed molecules and likely reduce the device performance and cost effectiveness. Therefore, more study is needed to solve these issues. A second approach is to introduce additive molecules, such as C_{60},[4] $PC_{71}BM$,[15] or polymer,[16] into the active layer to suppress the crystallization of PCBM. With these additives, micro-scale phase separation was not observed even after heating for a long time. In any event, the industrial manufacturing process of organic solar cells always involves many thermal processes at high temperatures,[17] whereas none of the existing approaches maintain the stability of the devices throughout prolonged thermal annealing, thus leading to highly reduced efficiency.[4,11,12,16]

In the present study, we demonstrate that the thermal stability of inverted organic photovoltaic (OPV) devices may be easily controlled by introducing Pc into the active layer of P3HT and PCBM. During the thermal annealing process, the Pc in the P3HT:PCBM blends suppressed the crystallization of P3HT and PCBM, as was confirmed by optical microscopic images and UV-visible absorption spectra. We also show the photovoltaic parameters of all devices as a function of aging time at 120 °C. The mechanism underlying the thermal stabilization of inverted solar cells via Pc will be discussed below.

2 Results and Discussion

The OPV devices were fabricated with the structure ITO/ZnO/P3HT:PCBM:Pc/PEDOT:PSS/Ag (Figure 1). In the first set of experiments, we used a blend of P3HT:PCBM:Pc (1:1:0.3) (w/w) dissolved in chlorobenzene to fabricate the active layer of the OPVs. A pristine P3HT:PCBM (1:1) mixture without Pc was used to fabricate the reference devices. To test the thermal stability, both reference devices and Pc-containing devices were

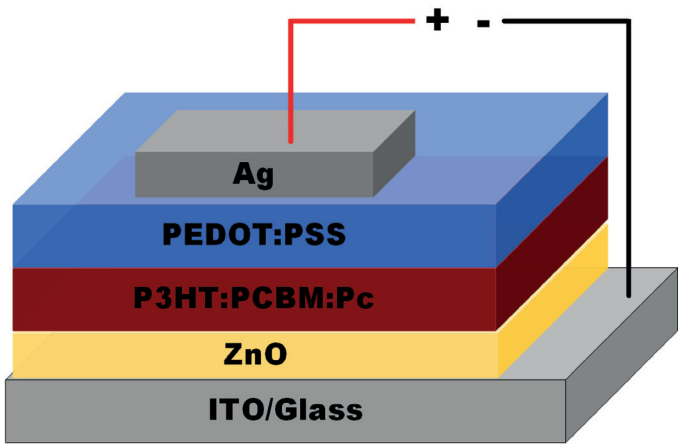

Figure 1. Schematic representation of the structure of an inverted polymer solar cell device.

aged at 120 °C for 0, 2, 6, 12, and 24 hours on a hot plate. The current density-voltage (*J-V*) characteristics of the reference device and Pc device (1:1:0.3) after aging are shown in Figures 2a and 2b, respectively. The corresponding photovoltaic parameters (PCE, open circuit voltage [V_{OC}], short circuit current density [J_{SC}], and fill factor [FF]) are summarized in Table 1. As illustrated in Figure 2a, the performance of the reference device dramatically decreased as the aging time increased. The PCE of the device dropped from 4.10 % to 1.07 % after aging for 12 hours. The decrease in efficiency comes from the decrease in J_{SC}, V_{OC}, and FF. In sharp contrast, the Pc-blended device showed very stable *J-V* characteristics and only degraded from 3.75 % to 3.49 % after being annealed for 12 hours (Figure 2b). The efficiency degradation of the Pc-containing device is mainly a result of the decrease in the J_{SC}. The properties of the Pc-containing device proved to be very stable and their values decreased very little even after long aging durations. We propose that the

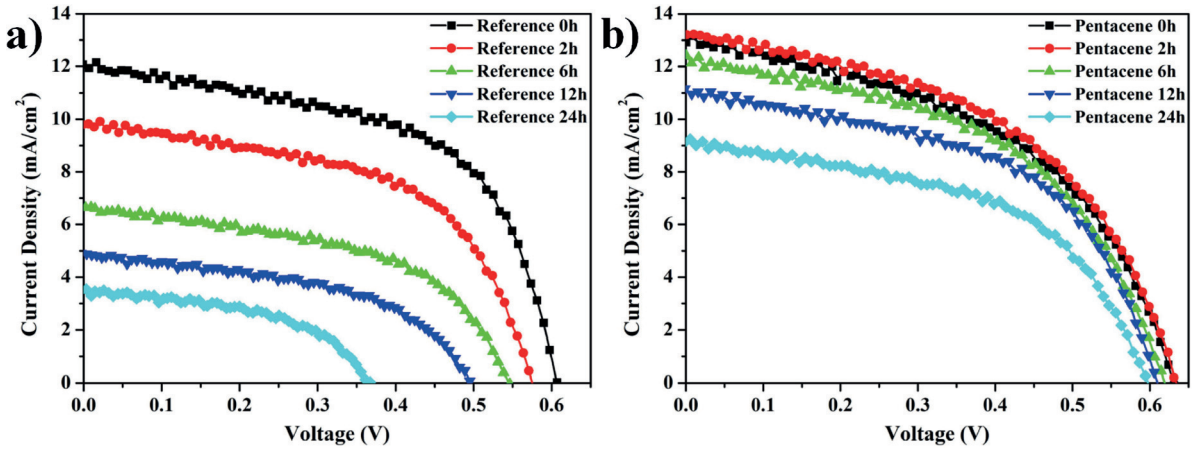

Figure 2. Current density-voltage characteristics of (a) reference devices and (b) Pc-containing devices (P3HT:PCBM:Pc = 1:1:0.3) after aging at 120 °C for 0 hours (0 h), 2 hours (2 h), 6 hours (6 h), 12 hours (12 h), and 24 hours (24 h) under illumination of AM1.5G, 100 mW/cm^2.

Table 1. Photovoltaic parameters of reference devices and Pc-containing devices (P3HT:PCBM:Pc = 1:1:0.3) as a function of aging time at 120 °C. The standard deviation in brackets and the average performance were calculated based on four devices.

Devices	Aging Time [h]	J_{SC} [mA/cm^2]	V_{OC} [V]	FF	PCE [%]
Reference	0	11.96 (±0.45)	0.61 (±0.00)	0.57 (±0.01)	4.10 (±0.13)
	2	9.73 (±0.11)	0.58 (±0.00)	0.55 (±0.00)	3.08 (±0.04)
	6	6.85 (±0.44)	0.54 (±0.00)	0.50 (±0.00)	1.88 (±0.12)
	12	4.55 (±0.31)	0.49 (±0.01)	0.48 (±0.01)	1.07 (±0.10)
	24	3.28 (±0.52)	0.36 (±0.02)	0.48 (±0.00)	0.56 (±0.12)
Pentacene	0	12.84 (±0.09)	0.63 (±0.01)	0.46 (±0.02)	3.75 (±0.18)
	2	13.10 (±0.37)	0.62 (±0.01)	0.49 (±0.01)	4.00 (±0.14)
	6	12.37 (±0.40)	0.62 (±0.00)	0.51 (±0.01)	3.49 (±0.19)
	12	11.15 (±0.50)	0.61 (±0.01)	0.51 (±0.01)	3.49 (±0.15)
	24	8.93 (±0.41)	0.60 (±0.01)	0.49 (±0.01)	2.65 (±0.17)

stable performance of these OPVs results from their donor-acceptor interface stabilization due to the introduction of Pc.

To further confirm the morphological effect of Pc in the active layer, we studied the optical microscopy of this layer. Optical images of spin-coated active layers with and without Pc on the ZnO/ITO glass substrates are shown in Figure 3a,d. The active layers of reference and Pc-containing devices were then thermally annealed in an oven at 160 °C for 10 min (Figure 3b,e). The devices were then aged at 120 °C for 24 hours on a hot plate, and the resulting optical images are shown in Figure 3c,f. The optical microscopic images of these active layers show a clear difference in morphology between the reference device and the Pc-containing device (Figure 3). There are many crystallites of PCBM on the surface of the active layer of the reference devices after thermal treatment. On the other hand, the surface of the active layer in Pc-containing devices is free of PCBM crystallites, even after aging at 120 °C for 24 hours.

Figure 3 also confirms that crystallization of PCBM in the P3HT:PCBM blend could easily occur after annealing at 160 °C for 10 min (Figure 3b) and that the overgrowth of PCBM crystallites continues during prolonged aging (Figure 3c). The length of the needle-like PCBM crystallites appeared to be approximately 120 μm after annealing. In Figure 3c, numerous smaller PCBM crystallites appear on the surface of the P3HT:PCBM blend after aging, beginning as nano-scale PCBM aggregates and growing into larger and visible crystallites. In contrast, introduction of Pc into the active layer very effectively suppresses the crystallization of PCBM. The active layer surfaces of Pc-containing devices are clear of PCBM crystallites despite thermal annealing and prolonged aging, as shown in Figure 3e,f. The addition of Pc to the P3HT:PCBM blend modified the growth kinetics of PCBM, thereby curbing the overgrowth of crystallites. We also confirmed this phenomenon using UV-Vis absorption spectra.

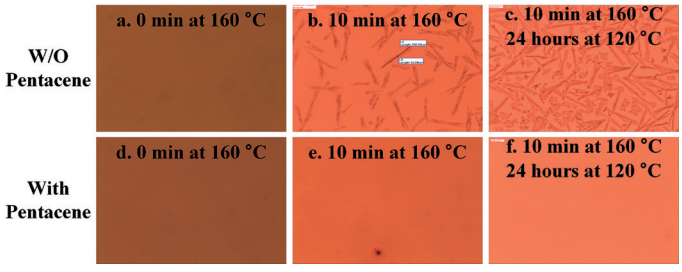

Figure 3. Optical microscopic images of the active layers of (a)–(c) reference devices (without [W/O] Pc) and (d)–(f) Pc-containing devices after thermal treatment under various conditions. Scale bar = 30 μm.

The effect of Pc on PCBM crystallization can be observed in the UV-visible absorption spectra in Figure 4. Comparing the absorption spectra of the active layers of reference and Pc-containing devices, there was a clear decrease in the absorbance of the reference device at a wavelength of 336 nm. This peak is the lowest energy

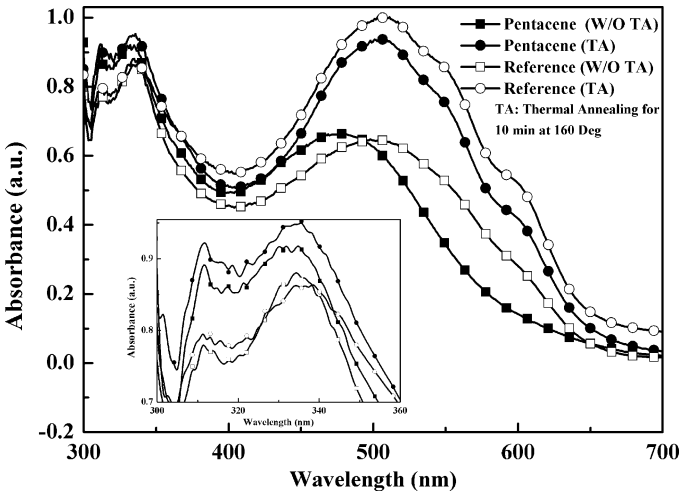

Figure 4. UV-Vis absorption spectra of active layers of a reference device and a Pc-containing device (P3HT:PCBM:Pc = 1:1:0.3). Spectra of both the as-produced films without (W/O) thermal annealing (TA) and the films after a thermal annealing for 10 min at 160 °C are shown. Inset: enlarged absorption spectra from 300–400 nm.

absorption feature for PCBM, and its decrease indicates migration of the isolated PCBM molecules to join large PCBM crystallites.[9] The absorbance of the unannealed active layer of the Pc-containing device (P3HT:PCBM:Pc = 1:1:0.2; solid squares) is higher than that of the reference device (P3HT:PCBM = 1:1; open squares) at 336 nm. This increase indicates that the suppression of PCBM crystallization in the Pc-containing device is initiated during the spin-coating of the active layer before any thermal treatment. Also, a comparison between the unannealed active layers of each type of device reveals a blue shift for the Pc-containing device in the absorption region of P3HT at 400–600 nm. This blue shift occurred due to the presence of Pc. After annealing at 160 °C for 10 min, the absorbance at 336 nm did not change much for either device, but the absorbance in the 400–600 nm region (i.e., the absorption region of P3HT) greatly increased. The thermal annealing of the active layer enhanced the absorption of incident light, thereby increasing the performance of the OPVs. The absorbance of the reference device (open circles) was slightly higher than that of the Pc-containing device (solid circles) after the thermal annealing. This increase is expected, as the large PCBM crystallites block or scatter a larger fraction of the incident light at all wavelengths, the result of which is a higher absorbance background. Interestingly, there is no evident absorbance of Pc at 660 nm[18] in the Pc-containing device.

To study the effect of different concentrations of Pc on the performance of OPVs, we varied the ratio of P3HT:PCBM:Pc in the mixture used during OPV fabrication according to 1:1:x (x = 0, 0.2, 0.3) (w/w) and studied the resulting effect. The thermal stability of the Pc-containing devices increased as the Pc content in the active layer increased. All the photovoltaic parameters of these three types of devices, as a function of aging time at 120 °C, are shown in Figure 5. The Pc-blended OPVs of ratio 1:1:0.2 show the best PCE at 4.35 %. The devices with blending ratio 1:1:0.3 and reference devices had peak efficiency values of 4.00 % and 4.10 %, respectively. However, the 1:1:0.3 Pc-containing devices achieved 71 % of their original PCE after aging at 120 °C for 24 hours, whereas the reference devices (1:1:0) were at 13 % of their original PCE. As shown in Figure 5a, the

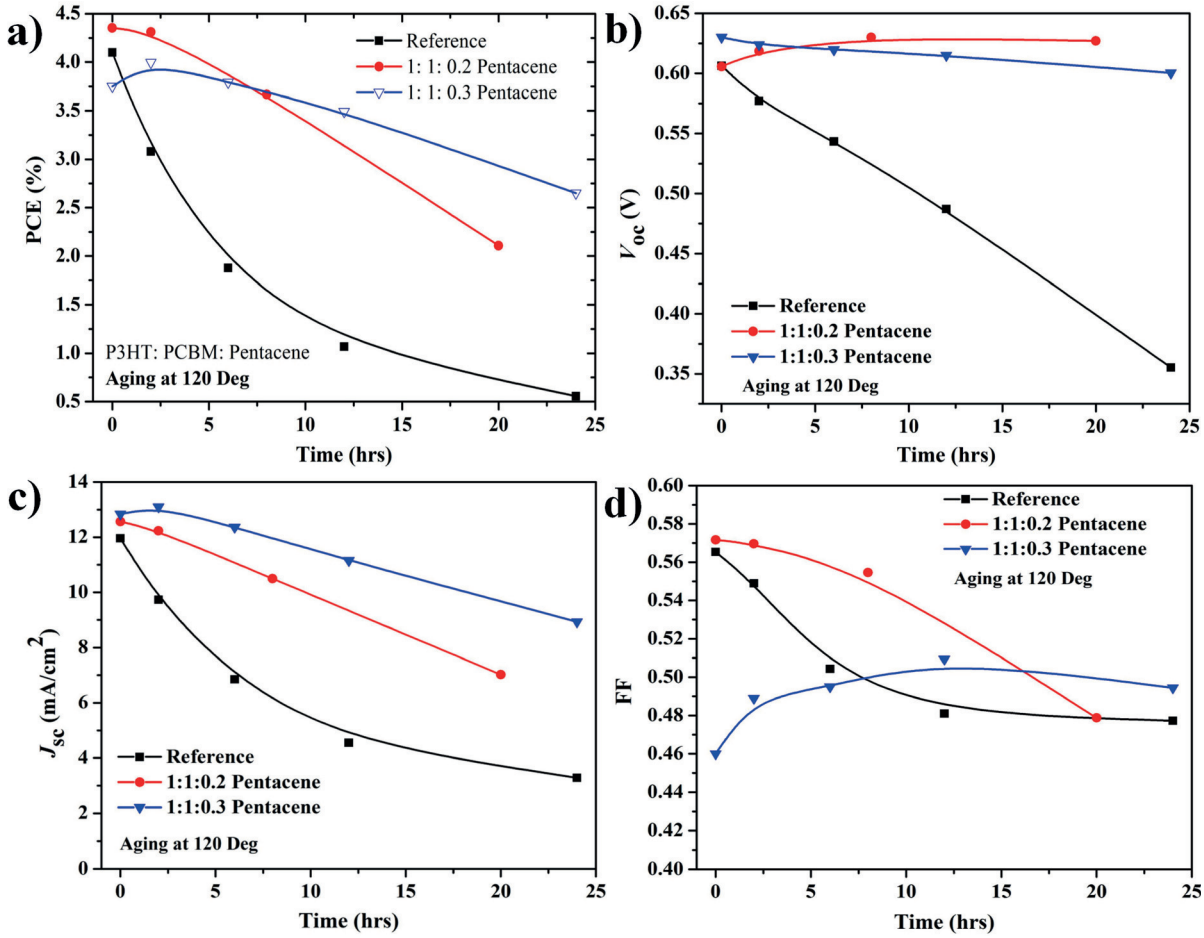

Figure 5. Photovoltaic parameters (a) PCE, (b) V_{OC}, (c) J_{SC}, and (d) FF of an OPV reference device and two Pc-containing devices, in which P3HT:PCBM:Pc = 1:1:0.2 and 1:1:0.3, respectively, as a function of aging time at 120 °C.

performance of Pc-containing devices, including blending ratios 1:1:0.2 and 1:1:0.3, were thermally stable and produced a PCE value of 3.7% after aging for 8 hours at 120 °C, while that of reference devices decreased dramatically to 1.6% under these conditions. Plots of FF, V_{OC}, and J_{SC} versus aging time for all the cases are displayed in Figure 5b–d. The decreased performance of reference devices was due to the rapidly deteriorating J_{SC}, V_{OC}, and FF, as shown in Figure 5b–d. The donor-acceptor interfaces of reference devices were badly coarsened during a long aging process, leading to rapid decrease in all photovoltaic parameters. In contrast, the V_{OC} values of Pc-containing devices were more thermally stable, and J_{SC} decreased slowly under thermal annealing, as shown in Figure 5b–c. The higher short-circuit current density (J_{SC}) observed for Pc-containing devices prior to aging indicates that the phase separation of donor and acceptor was properly controlled by the effect of Pc on PCBM. The improved interfaces of donor and acceptor could benefit the generation and separation of hole-electron pairs, which results in a higher J_{SC}. In addition, the hole transport property of Pc is better than that of P3HT, which explains the improved J_{SC} of solar cells with Pc. The stable V_{OC} and slowly decreasing J_{SC} indicate that the donor-acceptor interfaces of the active layer in Pc-containing devices were fixed by the effect of pentacene on crystallization of PCBM.

The thermal stability of inverted polymer solar cells could be enhanced by the effect of Pc on the crystallization of PCBM. We suggest that the π-π interaction between the PCBM and Pc is likely responsible for this effect. PCBM is a spherical molecule with many π electrons on its surface. Nano-scale ordered PCBM aggregates form very easily, even in the amorphous film. However, Pc also has π electrons, which compete and weaken the interaction among PCBM molecules. Pc in the active layer would make it harder for PCBM crystallites to form during aging at high temperatures.

3 Conclusions

The thermal stability of inverted polymer solar cells could be enhanced by the effect of Pc on the crystallization of PCBM. We found that introducing Pc into the active layer had a dramatic effect on the growth of PCBM crystallites during thermal treatment processes. Pc can modify the growth kinetics of PCBM crystallites such that the micrometer-sized crystal overgrowth of PCBM does not occur, even during prolonged aging at a high temperature of 120 °C. The donor-acceptor interfaces of the active layer in Pc-containing devices were fixed by the effect of Pc on crystallization of PCBM. The device with a 1:1:0.3 P3HT:PCBM:Pc blend showed great thermal stability and degraded only 7% in PCE, from 3.75% to 3.49%, after aging for 12 hours at 120 °C. Based on this work, there is a window of opportunity for high temperature processing of organic solar cells. OPVs with Pc could be advantageous during thermal processes in mass production, such as roll-to-roll fabrication, spin-coating, ink jet printing, spray coating, and screen printing.

4 Experimental Section

Materials. P3HT was purchased from Rieke Metals. PCBM was purchased from Nano-C. Pentacene was purchased from Polysis, and conductive polymer PEDOT:PSS (ICP 1020) was supplied by Agfa Materials. The ITO used for solar cells was supplied by Fine Chemicals (South Korea) (15 Ω/square; 0.7 mm thickness) and was cut into 1.9 cm × 1.9 cm squares. Chlorobenzene (anhydrous; 99.9%) was supplied by Sigma Aldrich. Triton X-100 (extra pure) was supplied by Do Chemical Co., Ltd. Hexamethyldisilazane (HMDS) was supplied by AZ Electronic Materials (South Korea).

The fabrication and characterization procedure of the devices are as follows. The ITO substrates were ultrasonicated twice for 10 min in deionized water, then in acetone, and then in isopropyl alcohol. A filtered ZnO precursor solution was then spin-cast onto cleaned ITO substrates at 8000 rpm for 20 s and then baked in an oven at 200 °C for 20 min. The thickness of the ZnO layer is ca. 40 nm. Next, 1:1:x (x = 0, 0.2, 0.3) (w/w) blends of P3HT:PCBM:Pc, with P3HT concentrations of 20 mg/ml, were dissolved in chlorobenzene by ultrasonication for 3 hours, filtered through a 0.45 μm PVDF filter, and spin-cast at 1000 rpm for 25 s onto the ZnO-coated ITO substrates. The formed active layer of P3HT:PCBM:Pc was 120–130 nm thick. In order to deposit hydrophilic PEDOT:PSS on the hydrophobic active layer, PEDOT:PSS was modified with 0.5% (v/v) of Triton X-100 nonionic surfactant. Also, HMDS was first spin-coated onto the active layer at 500 rpm for 5 s, followed by deposition of the modified PEDOT:PSS solution by spin-coating at 5000 rpm for 20 s. The films on substrates were annealed in an oven at 160 °C for 10 min. The thickness of PEDOT:PSS was 30–40 nm. The devices then underwent thermal deposition of ~100 nm Ag film through a shadow mask at a pressure of $\sim 6 \times 10^{-6}$ mTorr. Subsequently, the devices were aged on a hot plate at 120 °C for varying amounts of time. All fabrication processes were carried out in air, except for the thermal deposition process of Ag. Four devices per substrate were prepared, with an active area of 0.1 cm^2 per device. The *J-V* characterization of devices was carried out with *J-V curve tracer* (Eko MP-160) and a solar simulator (Yss-E40, Yamashita Denso) under AM1.5G (100 mW/cm^2) irradiation intensity calibrated by a Newport certified standard silicon cell. Absorption spectroscopic measurements were made over a wavelength range of 200–1000 nm using a Shimadzu UV-1601 UV-Vis spectrophotometer. Optical microscopic

images were obtained by using an Olympus BX41 microscope digital camera. The thicknesses of all films were measured by a surface profiler (Tencor Alpha-Step).

Acknowledgments

This work was supported by an international cooperation program managed by the National Research Foundation of Korea (No. 2014K2A2A2000803) and by the human resources development program of the Korea Institute of Energy Technology Evaluation and Planning (KETEP) grant (No. 20144030200580) funded by the Korean Ministry of Trade, Industry, and Energy.

References

[1] J. You, L. Dou, Z. Hong, G. Li, Y. Yang, *Prog. Polym. Sci.* **2013**, *38*, 1909.
[2] Z. He, C. Zhong, S. Su, M. Xu, H. Wu, Y. Cao, *Nat. Photonics* **2012**, *6*, 591.
[3] C. Chen, W. Chang, K. Yoshimura, K. Ohya, J. You, J. Gao, Z. Hong, Y. Yang, *Adv. Mater.* **2014**, *26*, 5670.
[4] C. Lindqvist, J. Bergqvist, C. Feng, S. Gustafsson, O. Backe, N. D. Treat, C. Bounioux, P. Henriksson, R. Kroon, E. Wang, A. S. Velasco, P. M. Kristiansen, N. Stingelin, E. Olsson, O. Inganas, M. R. Andersson, C. Muller, *Adv. Energy Mater.* **2014**, *4*, 1301437.
[5] A. J. Moule, K. Meerholz, *Adv. Mater.* **2008**, *20*, 240.
[6] S. S. Bavel, E. Sourty, G. de With, J. Loos, *Nano Lett.* **2009**, *9*, 507.
[7] S. Bertho, G. Janssen, T. J. Cleij, B. Conings, W. Moons, A. Gradisa, J. DHaen, E. Goovaerts, L. Lutsen, J. Manca, D. Vanderzande, *Sol. Energy Mater. Sol. Cells* **2008**, *92*, 753.
[8] J. Kesters, S. Kudret, S. Bertho, N. V. Brande, M. Defour, B. V. Mele, H. Penxten, L. Lutsen, J. Manca, D. Vanderzande, W. Maes, *Org. Electron.* **2014**, *15*, 549.
[9] J. J. Richards, A. H. Rice, R. D. Nelson, F. S. Kim, S. A. Jenekhe, C. K. Luscombe, D. C. Pozzo, *Adv. Funct. Mater.* **2013**, *23*, 514.
[10] H. C. Wong, Z. Li, C. H. Tan, H. Zhong, Z. Huang, H. Bronstein, I. Mcculloch, J. T. Carbral, J. R. Durrant, *ACS Nano* **2014**, *8*, 1297.
[11] H. J. Kim, A. R. Han, C. H. Cho, H. Kang, H. H. Cho, M. Y. Lee, J. M. J. Frechet, J. H. Oh, B. J. Kim, *Chem. Mater.* **2012**, *24* (1), 215.
[12] C. Y. Nam, Y. Qin, Y. S. Park, H. Hlaing, X. Lu, B. M. Ocko, C. T. Black, R. B. Grubbs, *Macromolecules* **2012**, *45* (5), 338.
[13] C. H. Hsieh, Y. J. Cheng, P. J. Li, C. H. Chen, M. Dubosc, R. M. Liang, C. S. Hsu, *J. Am. Chem. Soc.* **2010**, *132* (13), 4887.
[14] A. Diacon, L. Derue, C. Lecourtier, O. Dartel, G. Wantz, P. Hudhomme, *J. Mater. Chem. C* **2014**, *2*, 7163.
[15] C. Lindqvist, J. Bergqvist, O. Bache, S. Gustafsson, E. Wang, E. Olsson, O. Inganas, M. R. Andersson, C. Muller, *Appl. Phys. Lett.* **2014**, *104*, 153301.
[16] L. Zheng, J. Liu, Y. Sun, Y. Ding, Y. Han, *Macromol. Chem. Phys.* **2012**, *213*, 2081.
[17] M. Jorgensen, K. Norrman, S. A. Gevorgyan, T. Tromholt, B. Andreasen, F. C. Krebs, *Adv. Mater.* **2012**, *24*, 580.
[18] J. Hwang, C. D. Sunesh, M. Chandran, J. Lee, Y. Choe, *Org. Electron.* **2012**, *13*, 1809.

Received: December 31, 2014
Accepted: February 23, 2015
Published online: April 23, 2015